International Journal of Electrical, Electronic and Communication Sciences
ISSN: 2517-9438
Vol:3, No:5, 2009

# Dynamic Performances of Tubular Linear Induction Motor for Pneumatic Capsule Pipeline System

Wisuwat Plodpradista

***Abstract*—** Tubular linear induction motor (TLIM) can be used as a capsule pump in a large pneumatic capsule pipeline (PCP) system. Parametric performance evaluation of the designed 1-meter diameter PCP-TLIM system yields encouraging results for practical implementation. The capsule thrust and speed inside the TLIM pump can be calculated from the combination of the PCP fluid mechanics and the TLIM equations. The TLIM equivalent circuits derived from those of the conventional three-phase induction motor are used as a model to predict the static test results of a small-scale PCP-TLIM system. In this paper, additional dynamic tests are performed on the same small-scale PCP-TLIM system with two capsules of different diameters. The behaviors of the capsule inside the pump are observed and analyzed. The dynamic performances from the dynamic tests are compared with the theoretical predictions based on the TLIM equivalent circuit model.

***Keywords*—**Pneumatic capsule pipeline, Tubular linear induction motor

## I. Introduction

THE existing large pneumatic capsule pipeline (PCP) systems, which use air to propel wheeled capsules carrying freight inside a pipeline, have limited throughputs. The limitation comes from the presence of intrusive blowers/ compressors capsule pumps. To improve existing PCP system throughput, non-intrusive tubular linear induction motor (TLIM) capsule pumps are needed. A TLIM capsule pump consists of two parts: the stator – a pipe section with three-phase windings embedded in laminated ferromagnetic core and the rotor – a two-layer-wall wheeled capsule, with ferromagnetic inner layer and conductive outer layer. The TLIM acting as a capsule pump will allow the capsules free passage through the pump, thereby increasing the system throughput.

References [1]-[3] study various aspects of employing a TLIM as non-intrusive capsule pumps for large PCP systems. The necessary TLIM equations and the PCP fluid mechanics equations can be found in [2] and more detailed in [4]. Reference [4] also describes the PCP-TLIM design procedures using the derived PCP fluid mechanics and the TLIM equations. Reference [5] designs and analyzes a large PCP-TLIM system of 1-meter diameter. The most recent work is [6], which compares the results of the static tests performed on a small-scale PCP-TLIM system with the theoretical predictions calculated using the newly modified TLIM equivalent circuit models.

In this paper, the dynamic tests are performed on the small-scale 8”-diameter PCP-TLIM system found in [4] and [6] as shown in Fig. 1. The results obtained from the tests are used to verify the TLIM dynamic thrust and efficiency predictions calculated from the TLIM equivalent circuit model.

## II. TLIM Equivalent Circuit and Equations

The dynamic performance parameters, namely the electromagnetic thrust and efficiency of the TLIM capsule pump can be predicted and analyzed using basic equivalent circuit model. Only the equivalent circuit model representing a capsule inside the entire stator found in [6] with minor adjustment, as shown in Fig. 2, is used. The modification is done by inserting the core-loss resistance without rotor $R_0$ in parallel with the magnetizing reactance $X_m$. The reason for this modification is because the TLIM core-loss resistance has a relatively low value (relates to high core-losses) as can be seen from the static test results [6]. This adjustment in the equivalent circuit model representing a capsule inside the entire stator would yield better predictions.

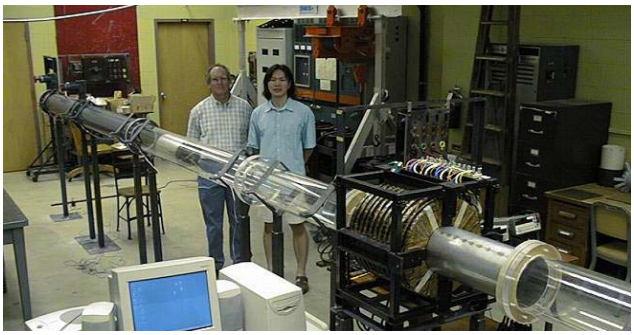

Fig. 1. The small-scale 8”-diameter PCP-TLIM system with the TLIM capsule pump located on the right. The TLIM stator has 12 slots and 4 poles.

W. Plodpradista is with the Department of Electrical and Electronics Engineering, the Faculty of Engineering, Assumption University, Bangkok 10250 Thailand (phone: 662-719-0480; fax: 662-719-1503; e-mail: wisuwatp@yahoo.com).

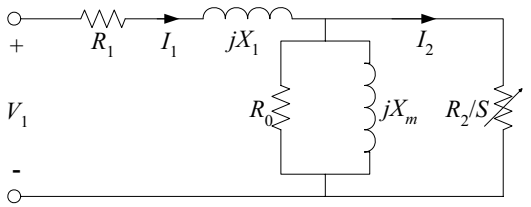


Fig. 2. The modified per-phase TLIM equivalent circuit with a capsule inside the entire TLIM stator.

### A. TLIM Equivalent Circuit Components

The components of the equivalent circuit model derived in [4] are given below.

*1) Per-Phase Stator Resistance:*

$$R_1 = \rho_w \frac{N_1 \pi (D + h_s)}{A_w}, \tag{1}$$

where $\rho_w$ is the volume resistivity of the copper wire used in stator winding, $N_1$ is the number of turns per phase, $D$ is the inner diameter of the TLIM bore, $h_s$ is the stator slot depth, and $A_w$ is the cross-sectional area of the wire.

*2) Per-Phase Stator-Slot Leakage Reactance:*

$$X_1 = 2\pi f \mu_0 W_s \frac{N_1^2}{pq} \frac{1}{pq_1} \left( \frac{h_s}{3w_s} \right), \tag{2}$$

where $f$ is the electrical frequency, $\mu_0$ is the permeability of free space, $W_s$ is the width of the TLIM ferromagnetic core, $p$ is the number of poles, $q$ is the number of slot-per-pole-per-phase, and $w_s$ is the stator slot width.

*3) Per-Phase Stator Core Loss Resistance without Rotor:*

$$R_0 = \frac{12 \rho_{Fe} A_c^2 k_w^2 N_1^2}{\pi^2 d_l^2 p^2 v_{core}}, \tag{3}$$

where $\rho_{Fe}$ is the volume resistivity of the ferromagnetic core, $A_c$ is the core cross-sectional area, $k_w$ is the winding factor for the fundamental harmonic of a full-pitch coil, $d_l$ is the core lamination thickness, and $v_{core}$ is the volume of the core.

*4) Per-Phase Magnetizing Reactance*:

$$X_m = \frac{2mf (k_w N_1)^2 \mu_0 L_s W_s}{\pi p^2 g_e}, \tag{4}$$

where $m$ is the number of phases, $L_s$ is the length of the TLIM stator core, and $g_e$ is the effective air gap found in [2]-[4].

*5) Per-Phase Rotor Resistance Referred to the Stator*:

$$R_2 = \frac{X_m}{G}, \tag{5}$$

where $G$ is the goodness factor defined as

$$G = \frac{2\mu_0 f \tau^2}{\pi (\frac{\rho_r}{d}) g_e}. \tag{6}$$

In (6), $\tau$ is the TLIM pole pitch, $\rho_r$ and $d$ are volume resistivity and thickness of the capsule conductor outer layer, respectively.

### B. TLIM Electromagnetic Thrust

In terms of the equivalent circuit components, the electromagnetic thrust generated by the TLIM can be found using the above-mentioned equivalent circuit model [2]-[4]. The TLIM thrust is

$$F_s = \frac{m I_1^2 R_2}{\left[ \frac{1}{(SG)^2} + 1 \right] V_s S}, \tag{7}$$

where $V_s$ is the TLIM synchronous velocity given as $V_s = 2f\tau$ and $S$ is the TLIM slip defined in [4].

### C. TLIM Capsule Pump Efficiency

The TLIM efficiency is calculated using the ratio of the output power developed by the capsule inside the TLIM stator to the input power consumed by the TLIM stator [4]. The output power developed by the capsule is

$$P_o = F_s V_c, \tag{8}$$

where $V_c$ is the capsule speed. The TLIM input power can be found from the TLIM thrust and the stator copper losses,

$$P_i = F_s V_s + m I_1^2 R_1. \tag{9}$$

## III. Dynamic Tests on Small-Scale PCP-TLIM System

The 8"-diameter small-scale PCP-TLIM laboratory system is 6.55 meters long and it is divided into four sections [4]. The first section consists of the inlet region for capsule loading and the TLIM capsule pump for thrust generation. The second section is for capsule deceleration after it exits the TLIM. The pipe in this section, which is transparent, is made of clear-cast acrylic for capsule observation. Next is the third section, which acts as the end zone for stopping the capsule. There are two air outlet lines with 2" PVC globe valves to control the airflow. By opening or closing these globe valves to different degrees, the flow resistance can be controlled to simulate various pipe lengths. The last section has an end plate mounted with an ultrasonic sensor to measure the capsule location at any given time. Along the pipeline, there are four pressure taps for measuring air pressure during capsule motion. Their locations are: P1 = 0.178 m down-stream from the TLIM stator exit,
P2 = 4.343 m down-stream from the TLIM stator exit,
P3 = 4.699 m down-stream from the TLIM stator exit,
P4 = 5.512 m down-stream from the TLIM stator exit.

The dynamic tests are designed to record the rms phase voltages, the rms phase currents, the three-phase TLIM input power, the capsule position while the capsule is moving inside the TLIM stator, and the gage pressures along the pipeline. The tests performed on the small-scale PCP-TLIM system are conducted using two capsules of different diameters. The capsule diameters are 7" (0.1778 m) and 7.125" (0.1810 m). The TLIM stator power supply is a three-phase 240 V rms line-to-line. The physical parameters of the small-scale PCP-TLIM system are given in Table I.

## IV. Test Results

The results from the dynamic tests are shown below. The figures are separated into two sets; Figs 3 to 8 belong to the 7"-diameter capsule while Figs 9 to 14 correspond to the 7.125"-diameter capsule. Note that only results with both air valves completely opened are shown in this paper.

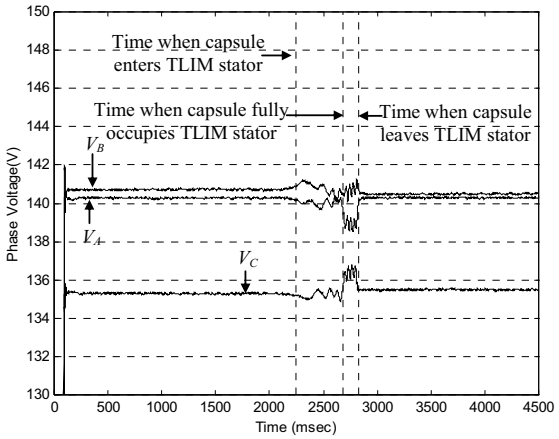


Fig. 3. The rms phase voltages vs. time for the 7”-diameter capsule with air valves completely opened.

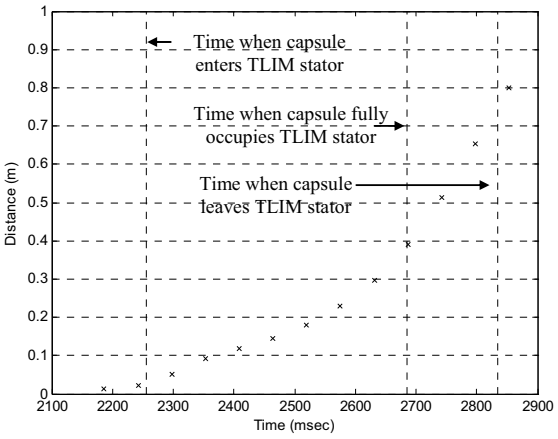


Fig. 6. The instantaneous capsule position inside the TLIM stator vs. time for the 7”-diameter capsule with air valves completely opened.

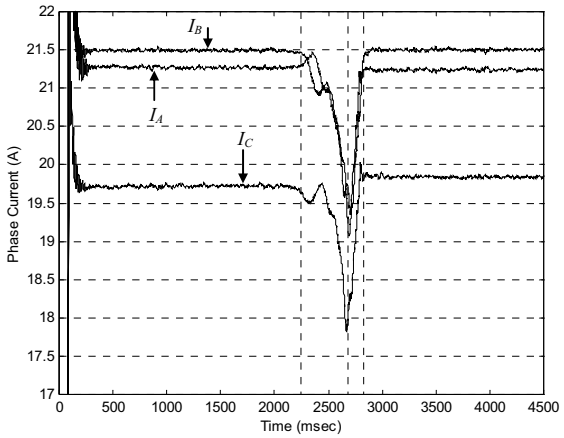


Fig. 4. The rms phase currents vs. time for the 7”-diameter capsule with air valves completely opened.

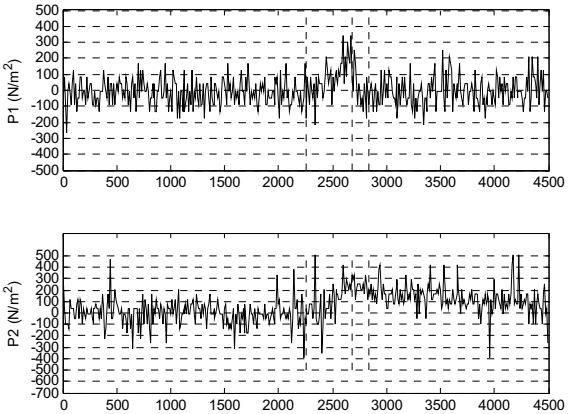


Fig. 7. Gage pressures at P1 and P2 vs. time for the 7”-diameter capsule with air valves completely opened.

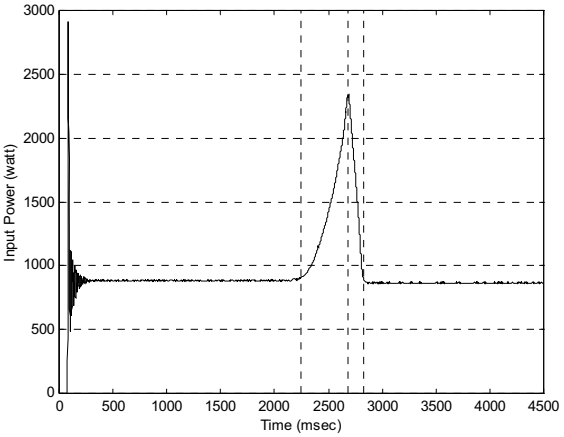


Fig. 5. The three-phase TLIM input power vs. time for the 7”-diameter capsule with air valves completely opened.

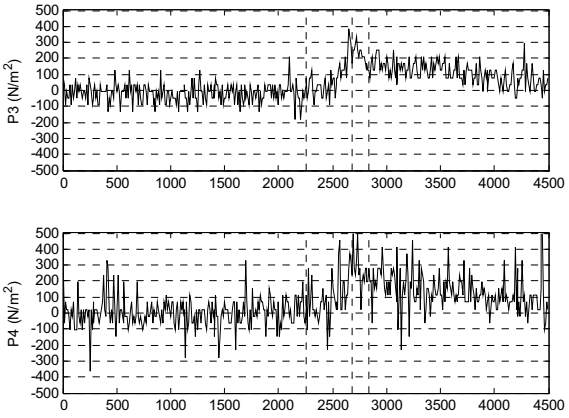


Fig. 8. Gage pressures at P3 and P4 vs. time for the 7”-diameter capsule with air valves completely opened.

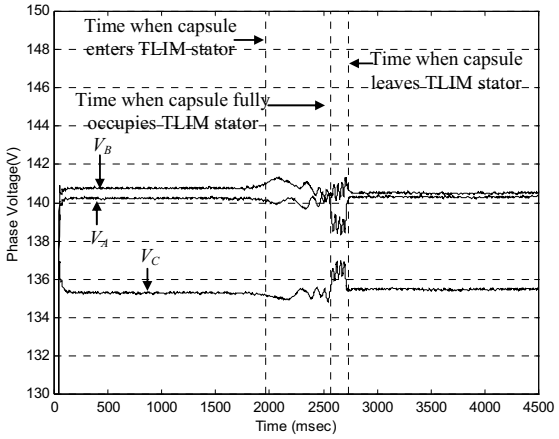


Fig. 9. The rms phase voltages vs. time for the 7.125”-diameter capsule with air valves completely opened.

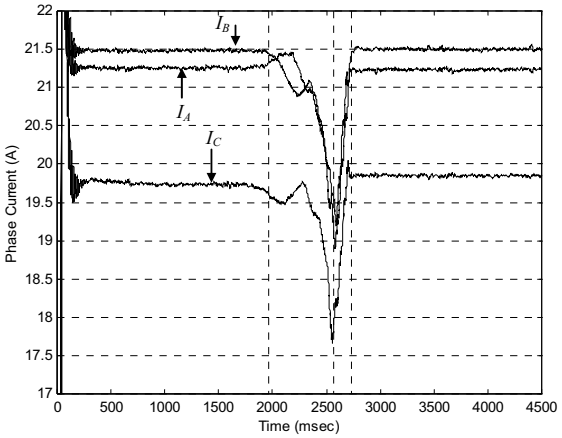


Fig. 10. The rms phase currents vs. time for the 7.125”-diameter capsule with air valves completely opened.

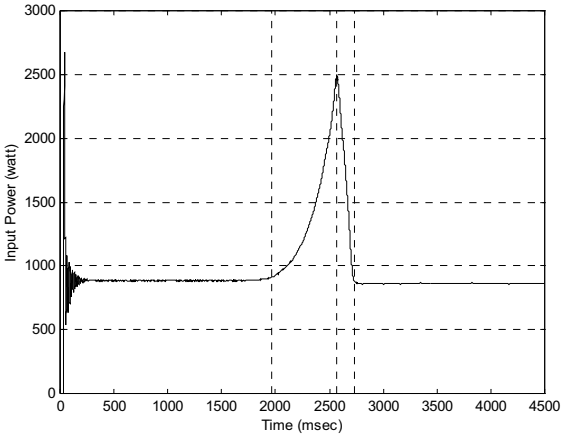


Fig. 11. The three-phase TLIM input power vs. time for the 7.125”-diameter capsule with air valves completely opened.

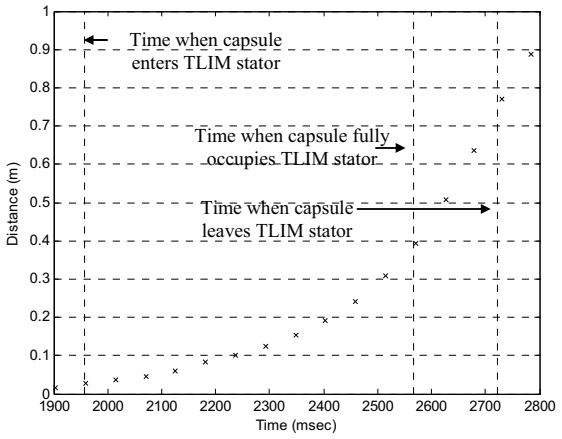


Fig. 12. The instantaneous capsule position inside the TLIM stator vs. time for the 7.125”-diameter capsule with air valves completely opened.

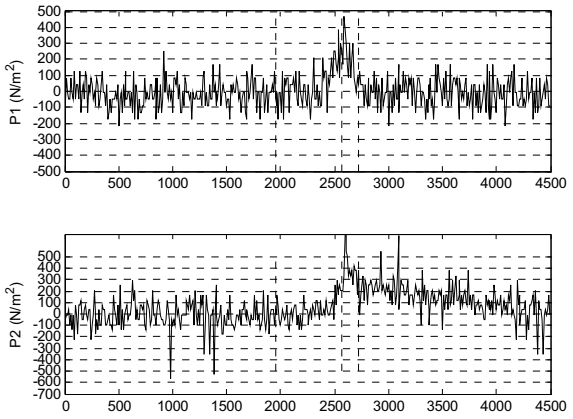


Fig. 13. Gage pressures at P1 and P2 vs. time for the 7.125”-diameter capsule with air valves completely opened.

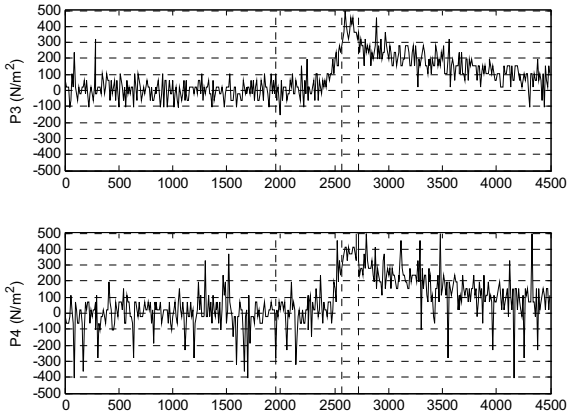


Fig. 14. Gage pressures at P3 and P4 vs. time for the 7.125”-diameter capsule with air valves completely opened.

TABLE I
THE SMALL-SCALE TLIM PHYSICAL PARAMETERS

| Description | Symbol | Value |
|---|---|---|
| TLIM stator bore diameter (m) | $D$ | 0.194 |
| Length of TLIM stator iron core (m) | $L_s$ | 0.360 |
| Width of TLIM stator iron core (m) | $W_s$ | 0.164 |
| Stator slot width (m) | $w_s$ | 0.015 |
| Stator slot depth (m) | $h_s$ | 0.100 |
| Thickness of capsule conductor outer layer (m) | $d$ | 0.0016 |
| Number of poles | $p$ | 4 |
| Number of turns per phase | $N_1$ | 240 |
| Number of slot-per-pole-per-phase | $q$ | 1 |
| Copper wire cross-sectional area ($mm^2$) | $A_w$ | 15 |
| Stator iron core cross-sectional area ($m^2$) | $A_c$ | 0.0192 |
| TLIM winding factor | $k_w$ | 1 |
| Stator iron core lamination thickness (mm) | $d_l$ | 1 |
| Stator iron core volume ($m^3$) | $v_{core}$ | $4.032 \times 10^{-3}$ |
| Copper volume resistivity (Ωm) | $\rho_w$ | $1.758 \times 10^{-8}$ |
| Iron core volume resistivity (Ωm) | $\rho_{Fe}$ | $2.500 \times 10^{-7}$ |
| Aluminum volume resistivity (Ωm) | $\rho_r$ | $3.447 \times 10^{-8}$ |
| Pole pitch (m) | $\tau$ | 0.09 |
| Electrical frequency (Hz) | $f$ | 60 |
| Synchronous velocity (m/s) | $V_s$ | 10.8 |

TABLE II
THE CAPSULES PHYSICAL PARAMETERS

| | | |
|---|---|---|
| Capsule diameter | 7” | 7.125” |
| Capsule mass (kg), $m_c$ | 9.5256 | 11.7963 |
| Friction force (N), $F_f$ | 4.00 | 4.89 |
| Capsule end disk cross-sectional area ($m^2$), $A_d$ | 0.0248 | 0.0257 |

The measured rms phase currents, shown in Figs. 4 and 10, decrease as the capsule enters the TLIM stator and have their minimum values when the capsule is entirely inside the stator. As the capsule exits the stator, the currents start to increase and return to their original level. This is because the presence of the capsule increases the equivalent TLIM impedance through the per-phase rotor resistance referred to stator $R_2$. The maximum value of $R_2$ occurs when the capsule is fully occupied inside the TLIM stator, hence the minimum rms phase current. Also note that the rms phase currents in the TLIM with the smaller capsule (7”-diameter) are higher because the smaller capsule has a larger physical air-gap. A larger air-gap leads to lower values of the per-phase magnetizing reactance $X_m$ and the per-phase rotor resistance referred to stator $R_2$. Lower values of $X_m$ and $R_2$ decrease the equivalent TLIM impedance, which eventually increases the rms phase current.

Unlike the rms phase currents, the three-phase TLIM input powers shown in Figs. 5 and 11, increase as the capsule enters the TLIM stator and peak when the capsule completely occupies the stator. This is to be expected since the TLIM stator should draw maximum input power when an entire capsule is inside the stator.

### A. Electromagnetic Thrust from Dynamic Tests

Since the electromagnetic thrust on the capsule cannot be measured directly, the recorded capsule position inside the TLIM are used to determine the measured TLIM dynamic thrust generated on the moving capsule inside the stator. The capsule drag force is found from the pressure data at either of the P1 or P3 locations, and the capsule acceleration equation is determined from the curve fitting equation match to the instantaneous capsule positions inside the TLIM stator. Recall that both the pressure data and the instantaneous capsule positions must be represented by equations established by curve fitting. The curve fitting equation for P1 or P3 discrete pressure data is a polynomial that fits the data in a least-squares manner. Similarly, the curve fitting equation for the instantaneous capsule discrete positions is also a polynomial.

The capsule drag force in the case of completely opened air valves is calculated from

$$F_d = P_1 A_d , \quad (10)$$

where $P_1$ is the gage pressure at P1 and $A_d$ is the capsule end disk cross-sectional area.

Once the drag force and the capsule acceleration are known, the measured TLIM dynamic thrust can be determined from

$$F_e = F_d + F_f + m_c a_c , \quad (11)$$

where $F_e$ is the measured TLIM dynamic thrust, $F_f$ is the friction force between the capsule wheels and the TLIM stainless steel bore, $m_c$ is the capsule mass, and $a_c$ is the capsule acceleration. The physical parameters of both capsules are shown in Table II.

The predicted TLIM dynamic thrust is calculated from the per-phase TLIM equivalent circuit with capsule inside the entire stator, as shown in Fig. 2. Since both the per-phase magnetizing reactance $X_m$ and the per-phase rotor resistance referred to stator $R_2$ derive from TLIM operation while a capsule occupies a full length of stator, the values of both components have to take into account the position of the capsule as it moves through the TLIM stator, i.e. when a portion of the capsule is inside the entire stator. For simplicity, it is assumed that these values are linearly proportional to the actual length of the capsule inside the TLIM stator. This active length is determined from the curve fitting equation of the instantaneous capsule position data. As the active length is determined at each instant of time, the predicted dynamic thrusts are calculated using Newton’s Laws with a 1-millisecond time interval.

### B. Comparison of the Measured and Predicted TLIM Dynamic Thrust and Efficiency

The plots of the measured and predicted dynamic thrusts and efficiencies are shown below. There are some errors between the predictions and measurements. This is because of the limitation of the equivalent circuit model used. It does not take into account many types of losses such as those occurred in the capsule end disks.

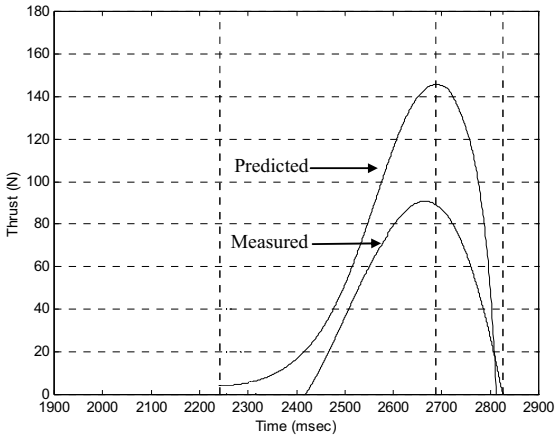


Fig. 15. The measured and predicted TLIM dynamic thrust vs. time for the 7"-diameter capsule with air valves completely opened.

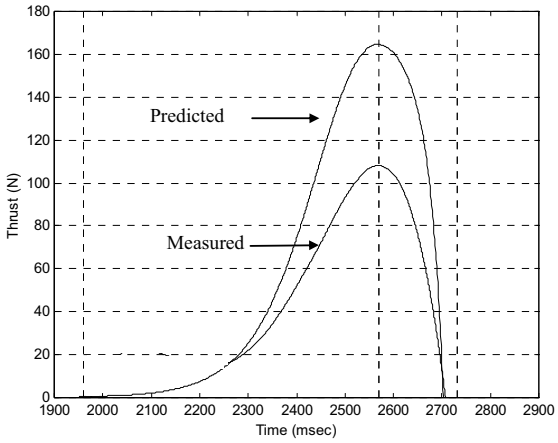


Fig. 17. The measured and predicted TLIM dynamic thrust vs. time for the 7.125"-diameter capsule with air valves completely opened.

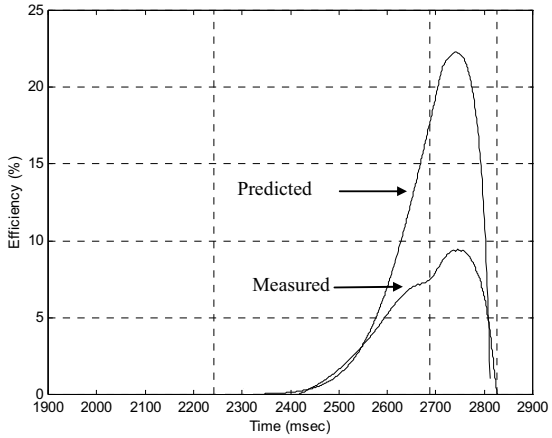


Fig. 16. The measured and predicted TLIM efficiency vs. time for the 7"-diameter capsule with air valves completely opened.

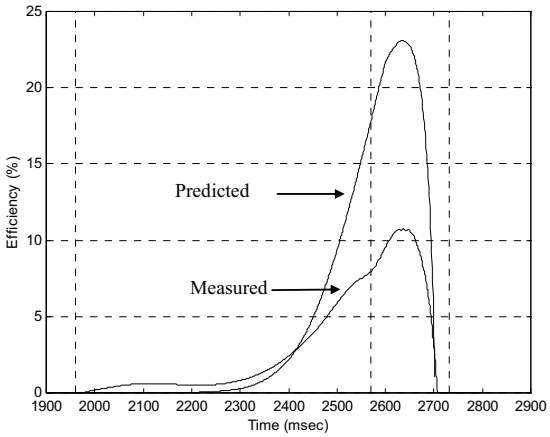


Fig. 18. The measured and predicted TLIM efficiency vs. time for the 7.125"-diameter capsule with air valves completely opened.

Figs. 15 and 17 show that the TLIM dynamic thrust peak approximately when the capsule fully occupies the stator. This is reasonable since the active length of the capsule is largest utilizing the total electromagnetic force generated by the TLIM stator. In contrast to the TLIM dynamic thrust, the TLIM efficiencies shown in Figs. 16 and 18 peak slightly after the point when the capsule is entirely inside and has begun to exit the stator. This is because the capsule velocity, which determines the TLIM output power, reaches its maximum point after the capsule fully occupies and has begun to leave the TLIM stator.

## V. Conclusions

This paper evaluates the dynamic performances of the small-scale PCP-TLIM system. The results from the dynamic tests are used to determine the TLIM dynamic thrust on the capsules. The TLIM theoretical predictions of the dynamic thrust and efficiency are calculated using the modified equivalent circuit model with a capsule inside the entire stator. The comparisons show that the modified equivalent circuit model can be used to satisfactory predict the TLIM dynamic thrust and efficiency for a PCP-TLIM system.

## References

[1] H. Liu, R. O'Connell, W. Plodpradista, and K. York, "Use of linear induction motors for pumping capsules in PCP," *Proc. of the 1st ISUFT*, Columbia, USA, pp. 84-94, 1999.

[2] W. Plodpradista and R. O'Connell, "Tubular linear induction motor design for pneumatic capsule pipeline systems," *Proc. of the 3rd IASTED International Conference PES '99*, Las Vegas, USA, pp. 252-256, 1999.

[3] H. Liu, "Improving economics of existing PCP system for transporting general cargoes," *Proc. of the 2nd ISUFT*, Delft, The Netherlands, 2000.

[4] W. Plodpradista, "Study of Tubular Linear Induction Motor for Pneumatic Capsule Pipeline System," Ph.D. dissertation, Department of Electrical Engineering, University of Missouri-Columbia, 2002, 202 pages.

[5] W. Plodpradista and R. O'Connell, "Design of a 1-meter tubular linear induction motor for a pneumatic capsule pipeline system," *Proc. of the 3rd ISUFT*, Bochum, Germany, 2002.

[6] W. Plodpradista, "Small-scale tubular linear induction motor for pneumatic capsule pipeline system," *Proc. of the ICEMS 2007*, Seoul, Korea, pp. 1528-1532, 2007.